

Evidence of Slumping/Sliding in Krishna-Godavari Offshore Basin due to gas/fluid movements

T. Ramprasad^{1*}, P. Dewangan¹, M.V. Ramana¹, A. Mazumdar¹, S.M. Karisiddaiah¹, E.R.

Ramya¹ and G. Sriram¹

¹National Institute of Oceanography, Dona Paula, Goa 403 004, India

(A constituent Laboratory of Council of Scientific and Industrial Research (CSIR), New Delhi)

*Corresponding author email: rprasad@nio.org

Abstract

The Krishna-Godavari (KG) offshore basin is one of the promising petroliferous basins of the eastern continental margin of India. Drilling in this basin proved the presence of gas hydrate deposits in the shallow marine sediments beyond 750 m water depths, and provided lithologic and stratigraphic information. We obtained multibeam swath bathymetry covering an area of about 4500 sq. km in water depths of 280 to 1800 m and about 1260 line km of high resolution seismic (HRS) records. The general lithology of mid-slope deposits is comprised of nannofossil-rich clay, nannofossil-bearing clay and foraminifera-bearing clay. The HRS records and bathymetry reveal evidence of slumping and sliding of the upper and mid slope sediments, which result in mass transport deposits (MTD) in the northwestern part of the study area. These deposits exhibit 3 - 9.5 km widths and extend 10 -13 km offshore. The boundaries of the MTDs are often demarcated by sharp truncation of finely layered sediments (FLS) and the MTDs are characterized by acoustically transparent zones in the HRS data. Average thickness of recent MTDs varies with depth, i.e., in the upper slope, the thickness is about 45 m, while in the lower slope it is about 60 m, and in deeper offshore locations they attain a maximum thickness of about 90 m. A direct indication for slumping and mass transportation of deposits is provided by the age reversal in ¹⁴C AMS dates observed in a sediment core located in the mid slope region. Seismic profiling signatures provide indications of fluid/gas movement. We propose that the presence of steep topographic gradients, high sedimentation rates, a regional fault system, diapirism, fluid/gas movement, and neotectonic activity may have facilitated the slumping/sliding of the upper slope sediments in the KG offshore basin.

1. Introduction

Mass flows/wastes, slides/slumps and slope instability on the continental margins have been reported worldwide. The main interest in studying such slides and slumps is due to their relation with the subsurface pressures which manifest in the form of fluid/gas expulsions. At the same time concerns are being raised due to the unforeseen geohazards caused by sliding/slumping, which affect the production platforms and other offshore engineering installations. The origin and causes of such submarine slides is yet to be established over the Indian continental margins. In general, instability of the slope sediments may result from high topographic gradient, large sediment influx, and high sedimentation rates. The movement of fluid/gas due to the presence of mud diapirs, regional fault system and neotectonic activity may weaken the sediment compressibility thereby facilitating the submarine slope failure. Further, the release of gas due to hydrate dissociation resulting from sea level fluctuations / neotectonic activity may enhance the likelihood of submarine slope failures. It is believed that gas hydrates have tremendous bearing in the seafloor instability (Carpenter, 1981; McIver, 1977, McIver, 1982; Booth et al., 1994). For example, the well known Storegga Slide, one of the largest submarine slides in the Norwegian continental margin appears to have been triggered by an earthquake combined with dissociation of gas hydrate (Bugge et al., 1987, Booth et al., 1994, Mienert and Posewang, 1999). The slope instability observed off New Zealand is caused by the gas hydrate "freeze-thaw" cycles (Pecher et al., 2008), led to dilation of fractures in mudstones in the Hikurangi Margin. Similarly, the Cape Fear Slide complex off North Carolina, US Atlantic Margin down slope is another example of occurrence of sliding/slumping (Schmuck and Paull, 1993). Ramana et al., (2007) interpreted few seismic sections and swath bathymetry in KG offshore basin and attributed the cause of the observed slumping structures to slope failure either by neotectonism or destabilization of gas hydrates due to fluctuations in sea level and rapid deposition of sediments. In the present study, we interpreted the high resolution sparker data under the constraints of geology and mapped mass transport deposits in KG offshore basin. We also made an attempt to understand the relationship between the observed MTD features to the regional fault systems, diapirism and the fluid/gas migration in KG offshore basin and explained the submarine slope failure through the geological processes.

2. Geological Setting

The eastern continental margin of India has evolved as a consequence of rifting and subsequent drifting of the Indian plate away from the contiguous Antarctica-Australia (Ramana et al., 2001). The Krishna-Godavari (KG) basin is a pericratonic basin extends to offshore. Its onland component spreads over 28,000 km² mostly covered by alluvium, while its offshore extent continues beyond the mid slope along the eastern continental margin of India, encompassing an area of

145,000 km². The basin is characterized by enechelon type horst and graben like structures, and the grabens are filled with a thick pile of Permian to Recent sediments (Rao, 2001; Rao and Mani, 1993; Gupta, 2006). Presence of gas hydrate in the Krishna-Godavari offshore basin has been confirmed by recent drilling (Collett et al., 2008), and the results indicated that this offshore basin is a well developed system for gas hydrate occurrence. It was predicted that regions surrounding the WNW-ESE trending sedimentary ridge in this offshore basin (cf. Fig. 2; Ramana et al., 2009) and particularly the northern sector of the ridge are the most promising zones for detailed gas hydrate exploration. The detailed analyses of multibeam bathymetry, high resolution sparker and multi-channel seismic data indicated several topographic mounds formed due to shale diapirism (Dewangan et al., 2010). The drilling/coring results onboard *DV JOIDES Resolution* and *MV Marion Dufresne* suggest that these mounds are probable locations for gas hydrate accumulation and formation of cold seeps in the KG offshore basin (Dewangan et al., 2010).

Godavari is the third largest river of India, and discharges a sediment load of ~153 million tons/yr, while the river Krishna carries about 102 million tons/yr (Sharma, 2002; Sarin et al., 2002). Both these rivers during relatively short monsoonal period produce significant annual discharge of sediment to the eastern continental margin of India, and it has been surmised that these sediment fluxes have continued since the genesis of the mighty Himalayas (late Miocene). The present day sea level was established about 5000 years ago and the progradation of the Krishna-Godavari delta has taken place since then with the seaward shift of the shore line until 800 years ago (Forsberg et al., 2007). Morphology of these delta fronts exhibit channel-levees with overbank and MTDs, scars and irregular topography features formed by sliding/slumping (Forsberg et al., 2007; Ramana et al., 2009). The sediments of widespread MTDs and submarine canyons over the modern upper continental slope in KG basin have been classified into: 1) sandy debrites, slump/slide cascading flows, 2) muddy slump and debrites, 3) sandy tidalite, 4) muddy tidalite, and 5) hemipelagite (Shanmugam et al., 2009).

3. Data

The geophysical (multibeam bathymetry and high resolution sparker) and geological (~30m long sediment cores) data were acquired onboard research vessels *ORV Sagar Kanya*, *RV Sagar Nidhi* and *MV Marion Dufresne* respectively under the gas hydrate exploration programme in the KG offshore basin (Fig.1) to study surface and subsurface geomorphological/geological features and their significance in gas hydrate detection as well as the processes responsible for their formation. The seafloor mosaic (Fig. 2) was generated from the multibeam bathymetry data after applying all the corrections. The single channel high resolution seismic (HRS) reflection data was acquired by deploying Geo-Spark 800 (High Resolution Sparker System). The sparker system works on the

principle of collapsing of the water bubble created by a high voltage electrical discharge. The high voltage power generator is capable of generating upto -5600 V with respect to ground and 10 kJ of power. A constant voltage of -4000 V and 5.6 kJ power was maintained throughout the cruise. The data were recorded using Geo-Trace 2 Data Acquisition System through a 24 element Geo-Sense single channel Streamer in GeoTrace Native format. The seismic data contains the frequency component of ~100-2000 Hz. The probable resolution of HRS data is between <8 to >100m depending on the nature of the shallow sediments.

The acquired data was converted to SEG-Y format and further processed using ProMAX 2D software at the computation centre of the National Institute of Oceanography (NIO), Goa. The data was displayed using amplitude attribute to enhance the quality of data for interpretation. Eight lines comprised of three SW-NE and five NW-SE lines are illustrated in the present study. A 28 m sediment core is used to study the physical properties of mass transport deposits. The wet bulk density of the whole core was measured onboard using the GEOTEK Multisensor Core Logger (MSCL) system following standard calibration and measurement protocol (www.geotek.co.uk/ftp/manual.pdf). The wet bulk density profiles are used to infer the variation in porosity and grain size of the shallow marine sediments. The foraminifera picked from sediment core at selected interval were dated using the AMS ¹⁴C facility at National Ocean Sciences AMS (NOSAMS), Woods Hole Oceanographic Institution, USA (<http://www.nosams.who.edu/clients/data.html>).

4. Results

4.1 Geomorphology

The study area (Fig.1) lies within the continental slope region of the KG offshore basin between the water depths of 400 and 1300 m with a variable gradient; 1:9 upper slope, 1:23 mid slope and 1:50 lower slope (Fig. 2). The swath bathymetry mosaic of the seafloor in general displays morphological features such as delta fronts, canyons, imprints of mud flow/pockmarks, scars/faults etc. The detailed interpretation of the bathymetry features in the KG offshore basin is provided by Ramana et al., (2009) and Dewangan et al., (2010). In this paper, we highlight four sediment mass flow-features including a secondary flow that are interpreted using swath bathymetry (Fig.2) and high resolution seismic data (Fig.3) in the continental slope region.

4.2 Description of subsurface features from HRS data

The HRS sections (Fig. 3) show that the upper ~35 m sequence comprises of finely layered sediments (FLS) in the northern part of the study area and such layering pattern is not observed beyond 700 m water depths. The FLS is defined to have a distinct bottom echo with several parallel,

continuous subbottom reflections that are conformable to the surface topography. In the northeastern and southwestern ends of the Line C, the sedimentary sequences are pierced by the diapiric structures (Fig. 3c). A similar subsurface diapir like structure is seen towards the northeastern end of the Line A (Fig. 3a). The surrounding overburden sediment sequences in the vicinity of these diapirs show amplitude blanking in the form of inverted U-shape/gas chimneys/pipe-like appearance (Fig.4a). These features in general vary in widths from <50 to ~100 m and ~75m by height (Fig.3). Hovland and Curzi, (1989) referred such features as acoustic voids. These acoustic voids/blanking zone/chimneys results from fluid/gas migration in the sediments. The HRS data depict a maximum sediment thickness of 475 m in the depocentre, and ~20 m in the lower slope region adjacent to diapir structures. Towards offshore (Figs. 3d, f), the pattern associated with FLS as mentioned above are absent, and we observed zones of acoustic transparent masses with no internal reflections. Such echo facies are commonly associated with mass transport deposits (Pratson and Laine, 1989). Occasionally, the FLS are seen truncated (Figs. 3a-d, f) followed by the acoustically transparent zone indicating that the strata have been disturbed by mass flows which is common phenomenon in the study area. The thickness of the inferred mass flow is ~60 m and extends laterally over 5 km within the water depths of 850 – 950 m. The detailed morphology of the mass transport deposits are illustrated in the zoom-out seismic sections of different lines in Figure 4b.

The mid slope region is characterized by a ~20 km wide marginal basin where sediment thickness attains a maximum of about 475 m. It is interesting to note the layering pattern in the syncline depicts two distinct characteristics of deposition (Fig. 3c). The sedimentary layers below the inferred LGM are influenced by tectonics and are manifested in the form of sagging, while the sedimentary layers above the LGM are least influenced by any recent tectonic activity. However, the internal configuration of these reflectors are characterised by varied thicknesses (10-40 m), and this variation may be due to differential sediment mass flow. The seismic reflector which separates these two distinct deposition patterns is undulatory and occasionally incised by channel/deep scars. In the deep offshore regions of mid slope an acoustically strong reflection mimicking the seafloor is conspicuous (Figs.3d, f, g). Since these subsurface reflections occur close to the base of the gas hydrate stability zone (NIO, 1997), we interpret these strong reflection zones as the Bottom Simulating Reflections (BSRs) which is the manifestation of gas hydrate and underlying free gas.

4.3 General lithology and age of the marker horizons

The lithology inferred from the sediment core (NGHP-01-03) has been superimposed on the seismic section close to the site (Fig. 3f). An average velocity of 1600 m/s derived from the well logs (Collett et al., 2008) is used for time-to-depth conversion. The lithology comprises of nannofossil-rich clay, nannofossil-bearing clay and foraminifera-bearing clay as per the IODP nomenclature. It is

interesting to note that the high reflective zones in the seismic records coincide with that of nannofossil-rich clay and the acoustically transparent zones represent nannofossil-bearing clay.

In order to estimate the approximate age of different horizons, we adopted variable sedimentation rates (0.25-1.0 m/ky) (Sarin et al., 1979, ONGC Personal Communication, Collett et al., 2008) and derived the tentative ages (0.35-1.4 my) of midslope sediments. We have recognized the Last Glacial Maximum (LGM, ~23,000 years) surface in the high resolution seismic data. The LGM surface is characterized by rugged/eroded surface, and occasionally incised by channel/deep scars (Figs.3a-c,f,g) which separates two distinct depositional patterns. Several distinct layer boundaries are observed within the sedimentary column from Quaternary to Recent. The seismic records depict the presence of MTDs (Figs. 3a,b,d-f) and these deposits are seen mostly above the LGM surface within the Holocene-Recent sediments. Interestingly, the older sediments are seen affected by the shale diapirism/mud flows, and this diapirism effect elevated the overlying sedimentary strata up to the seafloor. The LGM surface is overlain by distinct homogeneous sediment layers of ~10-15 m which may indicate that the transgression stage was dominated by a low energy environment in the study area.

4.4 Density profile

The density profile measured onboard *MV Marion Dufresne* of the sediment core (MD/161/11) located in the mid slope region of KG offshore basin is shown in Figure 5. The wet-bulk density of the sediment shows a normal density variation upto ~12 mbsf. However, we observed a periodic fluctuation in density (1.4-1.6 g/cc) below 12 m within the core. This density fluctuation can be inferred to be largely due to porosity variation as there is no major change in lithology. Figure 5 depicts four well defined periodic fluctuations in porosity i.e., (65-77 %) below 12 m. Although, grain size does not have a well established relationship with porosity as it depends on other significant factors such as grain shape and sorting but in general, grain size decreases as porosity increases (Hamilton, 1965). If we assume that the porosity increase is due to the decrease in grain size, then these porosity fluctuations can be interpreted as distinct fining upward sequences, a characteristic feature of turbidites deposits.

4.5 Radio Carbon Dating

The radiocarbon and calendar AMS ^{14}C dates of planktonic foraminifera (Table 1) show a uniform sedimentation rate of 2.1 m/kyr in the upper part (<12 mbsf) of the sedimentary column. Below 12 m, the sedimentation rate abruptly increases to > 40 m/kyr and age reversal is observed. We interpreted this abrupt increase in sedimentation rate along with age reversal (at ~15 mbsf) as a direct evidence of mass transport deposits.

5. Discussion

The submarine mass movements and their consequences are of major concerns for (i) coastal communities and infrastructure development along coastal corridors and (ii) exploration and development of marine resources. According to Burgess and Hovis (1988), transport of considerable sediment, including significant volumes of sand, into the deep marine realm via shelf-edge deltas is common during highstand time and may have enhanced by subsequent submarine canyon development.

The KG offshore basin is highly influenced by the huge sediment input since late Miocene, and the delta fronts developed during Holocene are incised by valleys and submarine canyons. The conventional multichannel seismic reflection data shows more than 7 km thick sediment overlying the early Cretaceous oceanic crust (Curry et al., 1982, Rao, 2001). We speculate that during a lowstand system tract with lower sea-level, the sediment depocentre may have reached the shelf edge as the shelf width is relatively small (~45 km). This results in accumulation of large volumes of sand and mud at the shelf edge.

5.1 Origin of mass wasting in KG offshore basin

Gas saturated sediments and sudden release of methane gas, dissociation of hydrate, high sedimentation rate and any tectonic (earthquake etc) activity are some of the factors that govern mass wasting/submarine slope failure. Rapid sedimentation on the shelf edge and upper slope during Pleistocene, and subsequent shift in the position of main depocentres coupled to the excess pore pressures due to the rapid sedimentation (Forsberg et al., 2007) resulted in slumping/sliding in the KG offshore basin (Bastia et al., 2007). A large submarine slide caused elsewhere by similar increase in sedimentation rate along with abundance of earthquakes is reported from the Bear Island Trough Mouth Fan, southwestern Barents Sea (Laberg and Vorren, 1993).

It is well established that the KG basin sediments show deformation styles related to gravity driven shale tectonism (Vijayalakshmi, 1988; Rao, 1993; Rao and Mani, 1993; Bastia, 2006; Gupta, 2006) and that shale diapirs are generated in the over pressured sequences of Upper Cretaceous, Paleocene, Eocene and Miocene. The folding and faulting of the overburden sediments are the result of shale diapirism / neotectonism, and some of these faults serve as natural pathways for the upward migration of fluid/gas. The occurrence of gas hydrate and presence of cold seeps (Mazumdar et al., 2009) are the testimony for the migration of fluid/gas. The surface expressions of the diapirism are manifested in the form of topographic mounds in the bathymetry data (Dewangan et al., 2010). In the present study, we have mapped the flow structures (i-iv), faults, topographic mounds, fluid/gas venting and the inferred head walls based on the HRS and bathymetry data (Fig. 6). The mounds associated with gas venting features (Figs. 3a,c,d,h) are related to subsurface shale diapirism. Numerous large-scale faults (Fig. 6) predominantly oriented in NNE-SSW and ENE-

WSW directions have been observed. Some of these faults have also been interpreted from the 3D seismic data in the western part of the study area (Reidel et al., 2010). The gas venting features disrupting the FLS observed from the seismic data coincide with some of the faults suggesting fluid/gas movements in the northern part of the study area.

From the HRS data (Figs.3 and 4), it is obvious that the slumping/sliding are closely associated with diapirism, faulting, and gas venting in the study area. Similar slumping/sliding due to gas/fluid venting near the diapiric structures have been reported from the Cape Fear submarine slide off Carolina (Schmuck and Paull, 1993). Another example of similar slumping is observed off Ratnagiri on the west coast of India due to the release of methane during Holocene (Gupta et al., 2002). We therefore believe that the high sediment influx, high sedimentation rate and steep seabed gradient initially cause the instability of the slope sediment. Further, the occurrence of fluid/gas venting associated with subsurface diapirism and regional fault system plays an important role in initiating the submarine slope failure in KG offshore basin.

The presence of gas hydrate has been reported in the KG Basin (Ramana et al., 2007). The gas hydrate stability conditions estimated from the available CTD profiles in the study area and the methane + seawater phase curve computed from the empirical formula given by Miles (1995) and NIO (1997) suggest that the gas hydrate are stable beyond 750 m water depths (Fig. 6). It is interesting to note that this boundary of gas hydrate forms a northern limit of the observed MTDs (flow structures caused by the sliding/slumping) designated as flow structures **i**, **ii**, **iii** and **iv**. Further, the gas venting features seem to cluster in shallow water depth (< 750 m) and their occurrence is relatively less in deeper depths. The dissociation of gas hydrate at the boundary of gas hydrate stability zone may have generated an excess pore pressure causing slope instability. The theoretical model developed by Sultan et al., (2004) shows that the origin of a retrogressive failure over Storegga Slope is due to the hydrate dissociation especially at the top of the hydrate stability zone (TGHS) contradictory to the beliefs that dissociation of hydrate occurs only at the bottom of the hydrate stability zone. Due to increase of temperature and pressure, the TGHS will move down leading to an increase of the methane solubility and consequently decomposing hydrate in a single-phase solution.

It is interesting to observe that most of the slumping/sliding is seen confined to the upper slope region only and not to the deep offshore region i.e., beyond 750 m water depths in the study area. At greater water depths the topography is gentle (1:50 gradient) with relatively lower sedimentation rate, which facilitates the stability of the sediment. The fluid/gas migrating from deeper horizons forms gas hydrate upon entering the hydrate stability zone. The presence of gas hydrate in the deep offshore region may provide additional strength to the sediment and thereby the sediment may be less susceptible to slumping/sliding.

6. Conclusions

We have mapped the prominent topographic mounds formed due to shale diapirism, fluid/gas expulsion zones, and regional fault system using multibeam swath bathymetry mosaic and high resolution seismic data in the study area. Several gas venting features such as inverted U-shaped zones and pipes displaying acoustic blanking of varying dimensions are observed in upper slope region (< 750 m water depth) suggesting the migration of fluid/gas through the upper slope sediments. The high resolution seismic reflection records under the constraint of swath bathymetry show the evidences of slumping / sliding predominant in the upper slope sediments. These mass transport deposits are 3-9.5 km wide and extend 10-13 km offshore. The boundaries of the MTDs are often demarcated by abrupt truncation of the finely layered sediment in the upper slope region (Fig. 4a). The high topographic gradient, high sedimentation rates and sediment influx in the upper slope region make the sediment unstable. The presence of fluid/gas in association with regional faults and subsurface diapirs may have enhanced the possibility of slumping/sliding in KG offshore basin. The reversal in ^{14}C AMS dates in KG offshore region further confirms the occurrence of slumping/sliding of the upper slope sediments. The correlation of lithology derived from sediment core (NGHP-01-03) with the HRS data suggests that the high reflective zones in the seismic records correspond to nanofossil-rich clay and the acoustically transparent zones represent nanofossil-bearing clay.

Acknowledgements

The Director of National Institute of Oceanography is thanked for the encouragement and the permission to publish. The Vessel Management Cell of National Institute of Ocean Technology, Chennai is thanked for providing the Research vessel Sagar Nidhi time for acquiring the HRS data. We profoundly thank the editor and anonymous reviewers for their critical reviews. NIO contribution No.

References

Bastia, R., Nayak, P., Singh, P., 2007. Shelf Delta to Deep Water Basin: A depositional model for Krishna-Godavari Basin, Search and Discover Article #40231, <<http://www.searchanddirectory.net/documents/2007/07011bastia/index.htm>>, accessed on Jan 16, 2010.

- Bastia, R., 2006. An overview of Indian sedimentary basins with special focus on emerging east coast deepwater frontiers, *The Leading Edge*, 25, 818-829.
- Booth, J.S., Winters, W.J., Dillon, W.P., 1994. Circumstantial evidence of gas hydrates and slope failure associations on the United States Atlantic continental margin, In: Sloan E.D., Happle J., Illnatow, M.A.(Eds.), *International conference on natural gas hydrates*, New York, Plenum Press, 487-489.
- Bugge, T., Befring, S., Belderson, R.H., Eidvin, T., Jansen, E., Kenyon, N.H., Holtedahl H., Serjup, H.P., 1987. A giant three-stage submarine slide off Norway, *Geo Marine Letters*, 7, pp. 191-198.
- Burgess, P.M., Hovius, N., 1988. Rates of Delta Progradation during highstands: consequence for timing of deposition in the deepmarine systems, *Journal of Geological Society, London*, 155, 217-222.
- Carpenter G., 1981. Coincident sediment slump/clathrates complexes on the US Atlantic continental slope, *Geo Marine Letters*, 1, 29-32.
- Collett et al., 2008. National Gas Hydrate Program Expedition 01 initial report, Director General of Hydrocarbons, Ministry of Petroleum and Natural Gas, New Delhi.
- Curry, J.R., Emmel, F.J., Moore, D.G., Raitt, R.W., 1982. Structure and geological history of Northern Indian Ocean, In: Nairn, A.E.M., Stehli, F.G. (eds.), *The Ocean Basins and Margins*, 6, 399-450.
- Dewangan, P., Ramprasad, T., Ramana, M.V. , Mazumdar, A., Desa, M., Badesab, F., 2010. Seabed Morphology and Gas Venting Features in the Continental Slope Region of Krishna-Godavari Basin, Bay of Bengal: Implications in Gas-Hydrate Exploration, *Marine and Petroleum Geology*, 27(7), 1628-1641.
- Forsberg, C.F., Solheim, A., Kvalstad, T.J., Vaidya, R., Mohanty, S., 2007. Slope instability and mass transport deposits on the Godavari river delta, east Indian margin from regional geological perspective, In: Lykousis, V., Sakellariou, Locat, J. (Eds.), *Submarine mass movements and their consequences*, 19-27.
- Gupta, M.V.S., Mohan, R., Muralinath, A.S., 2002. Slumping on the western continental margin of India, *GeoActa*, 1, 45-48.
- Gupta, S.K., 2006. Basin architecture and petroleum system of Krishna Godavari Basin, East Coast of India, *The Leading Edge*, 25, 830-837.
- Hamilton, E.L., and H. W. Menard, Density and porosity of sea-floor surface sediments off San Diego, California, *AAPG Bulletin* 1956 40: 754-761.

- Hovland M., Curzi, P.V., 1989. Gas seepage and assumed mud diapirism in the Italian central Adriatic Sea, *Marine and Petroleum Geology*, 6, 161-169.
- Laberg, J.S., Vorren, T.O., 1993. A Late Pleistocene submarine slide on the Bear Island Trough Mouth Fan, *Geo-Marine Letters*, 13, 227-234.
- Mazumdar, A., Dewangan, P., Joao, H.M., Peketi, A., Khosla, V.R., Kocherla, M., Badesab, F.K., Joshi, R.K., Roxanne, P., Ramamurty, P.B., Karisiddaiah, S.M., Patil, D.J., Dayal, A.M., Ramprasad, T., Hawkesworth, C.J., Avanzinelli, R., 2009. Evidence of paleo-cold seep activity from the Bay of Bengal, offshore India, *Geochemistry Geophysics Geosystems*, 10(6), 15 pp, doi:10.1029/2008GC002337.
- Mclver, R.D., 1977. Hydrates of natural gas - an important agent in geological processes, *Geol. Soc. America Ann. Mtg., Abs. with Programs*, 9, 1089-1090.
- Mclver, R.D., 1982. Role of naturally occurring gas hydrates in sediment transport, *AAPG Bulletin*, 66, 789-792.
- Mienert J., Posewang, J., 1999. Evidence of shallow- and deep-water gas hydrate destabilizations in North Atlantic polar continental margin sediments, *Geo-Marine Letters*, 19, 143-149.
- Miles, P. R., 1995. Potential distribution of methane hydrate beneath the European continental margins, *Geophysical Research Letters* 22(23), 3179-3182.
- NIO, 1997. Gas Hydrate Resource Map of India, NIO/SP-25/97, prepared for GAIL (India) Limited, 56pp.
- Pecher, I.A., Henrys, S. A., Ellis, S., Greinert, J., Chiswell, S.M., 2008. Erosion of Seafloor ridges at the top of the gas hydrate stability zone, Hikurangi margin, New Zealand - New insights from research cruises between 2005 and 2007, *Proceedings of the International Conference on gas hydrates (ICGH 2008)*, Vancouver, British Columbia, Canada, July, 6-10,2008, 10pp.
- Pratson, L.F., Laine, E.P., 1989. The relative importance of gravity-induced versus current-controlled sedimentation during the Quaternary along the mideast U.S. outer continental margin revealed by 3.5 kHz echo character, *Marine Geology*, 89, 87-126.
- Ramana, M.V., Krishna, K.S., Ramprasad, T., Desa, M., Subrahmanyam, V., Sarma, K.V.L.N.S., 2001. Structure and tectonic evolution of the northeastern Indian Ocean, In: SenGupta, R.; Desa, Ehrlich (Eds.), *The Indian Ocean: A perspective*, Oxford & IBH, New Delhi (India), 731-816.
- Ramana, M.V., Ramprasad, T., Kamesh Raju, K.A., Desa, M., 2007. Occurrence of gas hydrates along the continental margins of India, Particularly the Krishna-Godavari offshore basin, *International Journal of Environmental Studies*, 64(6), 675-693.

- Ramana, M.V., Ramprasad, T., Paropkari, A.L., Borole, D.V., Ramalingeswara Rao, B., Karisiddaiah, S.M., Desa, M., Kocherla, M., Joao, H.M., Lokabharati, P., Gonsalves, Maria-Judith, Pattan, J.N., Khadge, N.H., Prakash Babu, C., Sathe, A.V., Kumar, P., Sethi, A. K., 2009. Multidisciplinary investigations exploring indicators of gas hydrate occurrence in the Krishna-Godavari Basin offshore, east coast of India, *Geo-Marine Letters*, 29(1), 25-38
- Rao, G.N., 1993. Geology and hydrocarbon prospects of East Coast sedimentary basin of India with special reference to Krishna-Godavari Basin. *Journal of Geological Society of India* 41, 444-454.
- Rao, G.N., 2001. Sedimentation, stratigraphy, and petroleum potential of Krishna-Godavari Basin, East Coast of India. *AAPG Bulletin* 85, 1623-1643.
- Rao, G.N., Mani, K.S., 1993. A study on generation of abnormal pressures in Krishna-Godavari basin. *Indian Journal of Petroleum Geology* 2, 20-30.
- Riedel, M., Collett, T.S., Kumar, P., Sathe, A.V., Cook, A., 2010. Seismic imaging of a fractured gas hydrate system in the Krishna-Godavari Basin offshore India, *Marine and Petroleum Geology*, doi:10.1016/j.marpetgeo.2010.06.002.
- Sarin, M.M., Borole, D.V., Krishnaswami, S., 1979. Geochemistry and geochronology of sediments from the Bay of Bengal and the equatorial Indian Ocean, *Proceedings of Indian Academy of Sciences*, 88, 131-154.
- Sarin M.M., Sudheer, A.K., Balakrishna K., 2002. Significance of riverine carbon transport: a case study of a large tropical river, Godavari (India), *Science in China (Series C)*, 45, 97-108.
- Schmuck, E.A., Paull, C.K., 1993. Evidence for gas accumulation associated with diapirism and gas hydrates at the head of the Cape Fear Slide, *Geo-Marine Letters*, 13, 145-152.
- Shanmugam G., Shrivastava, S.K., Das, Bhagaban, 2009. Sandy debrites and tidalites of Pliocene reservoir sands in upper-slope canyon environments, offshore Krishna-Godavari basin (India): implications, *Journal of Sedimentary Research*, 79, 736-756, DOI:10.2110/jsr.2009.076.
- Sharma, K.P., 2002. A study of sediment fluxes to the coastal zone in south Asia and their relationships to human activities, Project Report on APN Project on a study of nutrient, sediment and carbon fluxes to the coastal zone in south Asia and their relationship to human activities, 20pp.
- Sultan, N., Cochonat, P., Foucher, J.P., Mienert, J., 2004. Effect of seafloor melting on seafloor instability, *Marine Geology*, 213, 379-401.
- Vijayalakshmi, K.G., 1988. Miocene depositional systems in thrust areas in Krishna-Godavari basin, *Bulletin of Oil and Natural Gas Corporation*, 25(2), 1-10.

Figure Captions

Figure 1. Map showing the available high-resolution seismic lines in the study area along with depth contours (25 m interval). The CDP numbers are annotated for each of the seismic profile. The solid circle represents the core location (Station 11 of *MV Marion Dufresne* Cruise 161) and a star representing the location of the drill core location (NGHP-01-03). The inset indicates the location of the study area.

Figure 2. Map showing the colour coded bathymetry with 50 m contour interval to highlight the sedimentary flow structures (i, ii, iii and iv). The delta front, head walls and diapiric structures are marked on the bathymetry map. The artificial lineations in the NE-SW direction observed in the map are due to the mismatch of depths along the track lines.

Figure 3 a) HRS section along Line A showing various subsurface features such as finely layered sediments (FLS), diapirs, faults, seismic signature of gas/fluid migration, the interpreted mass transport deposits (MTDs). In deep-offshore, an high amplitude reflection occurring close to the estimated base of the gas-hydrate stability zone is interpreted as Bottom Simulating Reflector (BSR), b) HRS section along Line B. c) HRS section along Line C d) HRS section along Line 1. e) HRS section along Line 2. f) The HRS section along Line 3 with the available lithology information from NGHP-01-03 site (Collett et al., 2008). g) HRS section along Line 4. h) HRS section along Line 5. Time-to-depth conversion is done assuming the sound velocity of 1500m/s. The locations of the seismic lines and the NGHP-01-03 site are shown in Figure 1.

Figure 4 a) Enlarged portions of the seismic sections to high light the FLS and seismic signatures of fluid/gas migration such as the inverted U-shapes, gas chimneys and vents, and pockmarks.

Figure 4 b) Enlarged portions of seismic sections to highlight the detailed morphology of MTDs. The boundaries of MTDs are identified by abrupt truncation of FLS.

Figure 5. Wet-bulk density, porosity and ^{14}C AMS dates of a long sediment core (~ 28 m) located in the mid slope region of KG offshore basin. The core location is shown in figure 1.

Figure 6. Summary map depicting the mounds formed due to shale diapirs, the sedimentary flow structures (i-iv), head walls (H1 & H2), regional fault system oriented predominantly in the NNE-SSW and ENE-WSW directions, boundary of the gas hydrate stability zone, and the available core locations The boundary of gas hydrate stability zone is marked by the 750m contour.

Table Caption

Table 1. Calendar age of a sediment core (MD161/11) located in mid slope region of KG offshore basin. The first occurrence of age reversal is highlighted at ~15 mbsf.

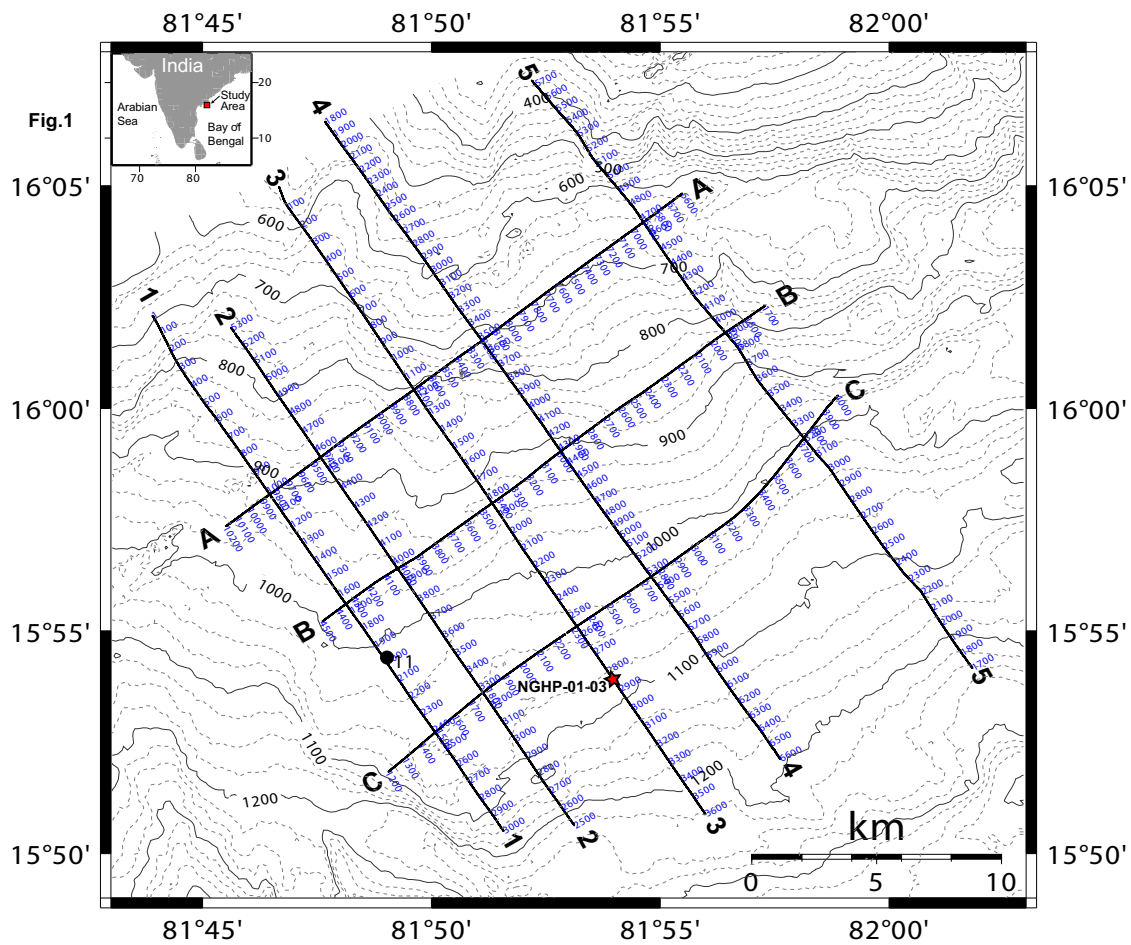


Fig.1

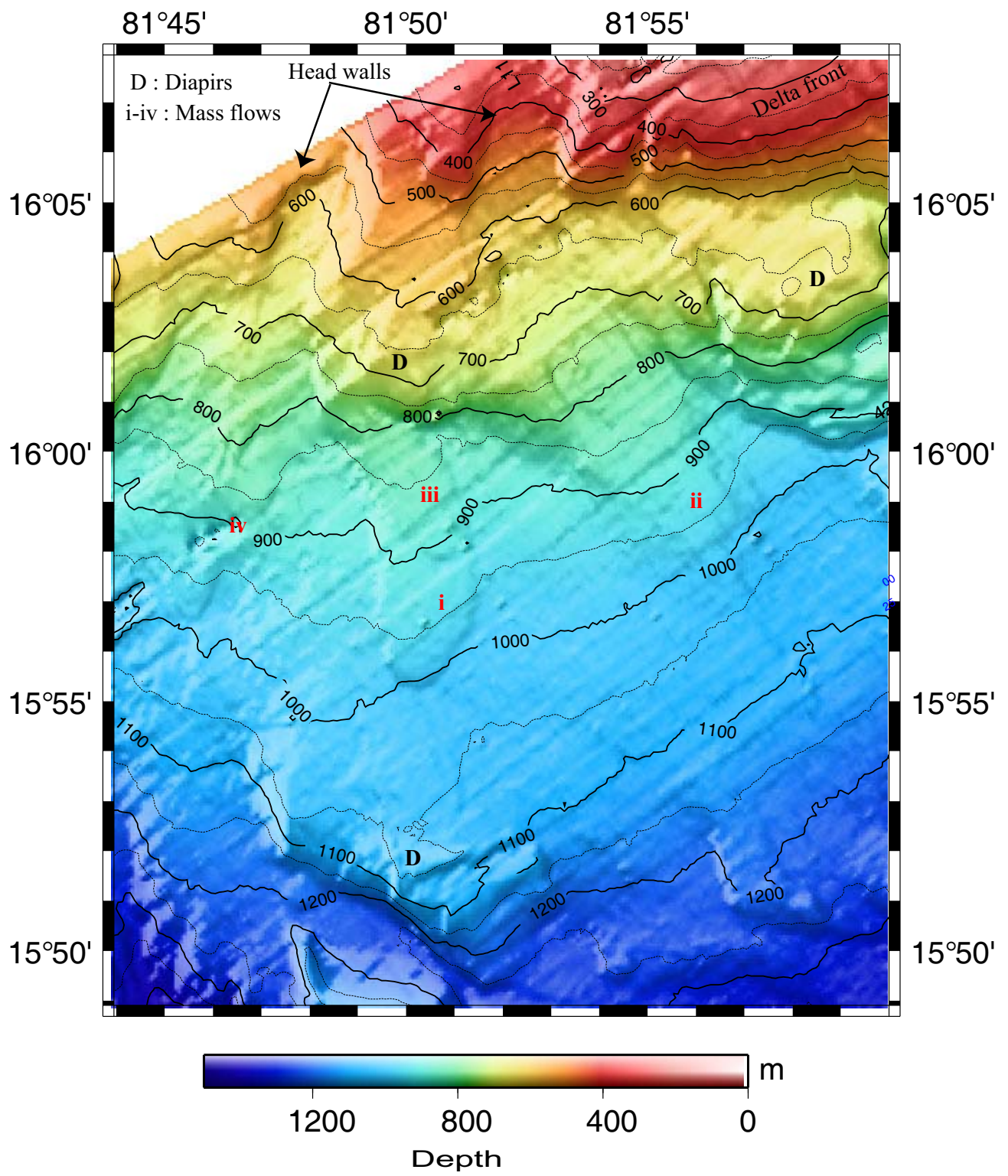
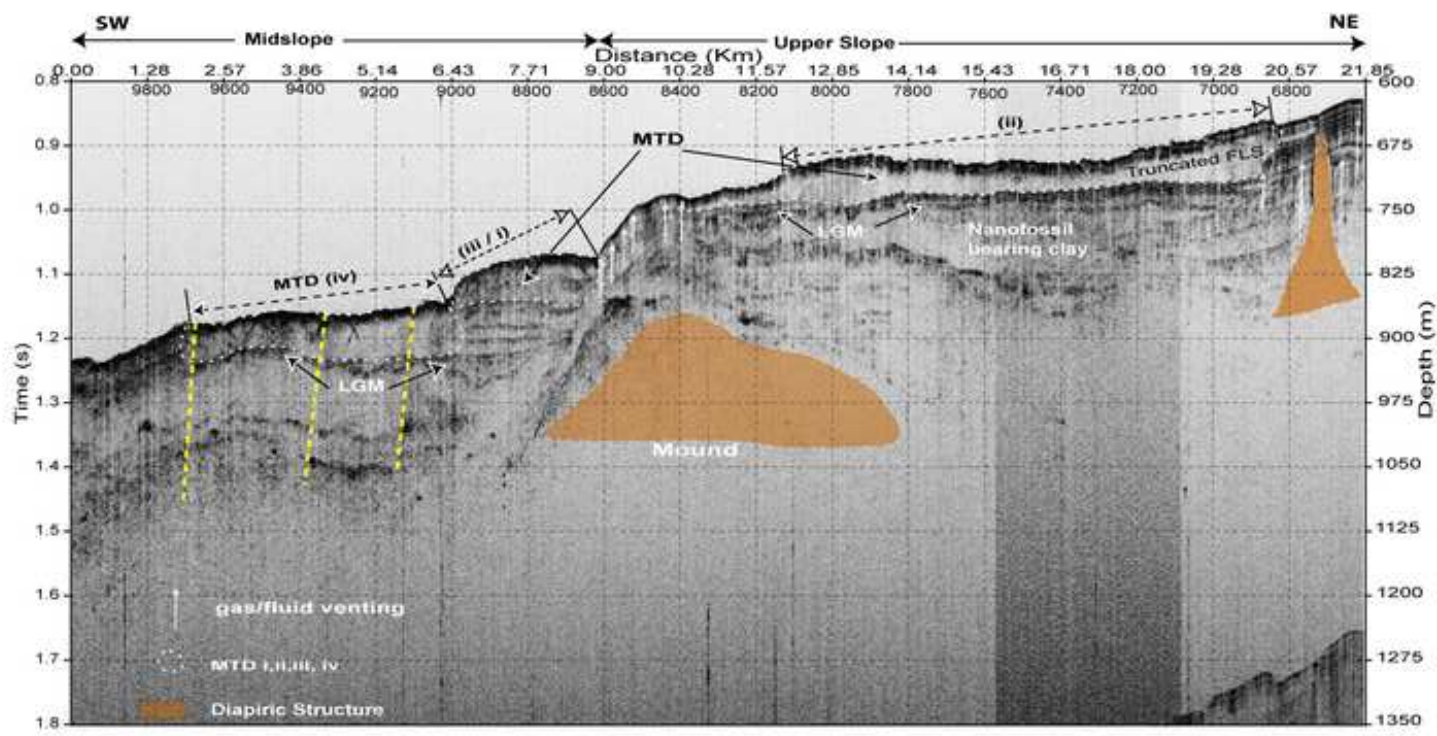


Fig. 2



Line A

Fig.3a

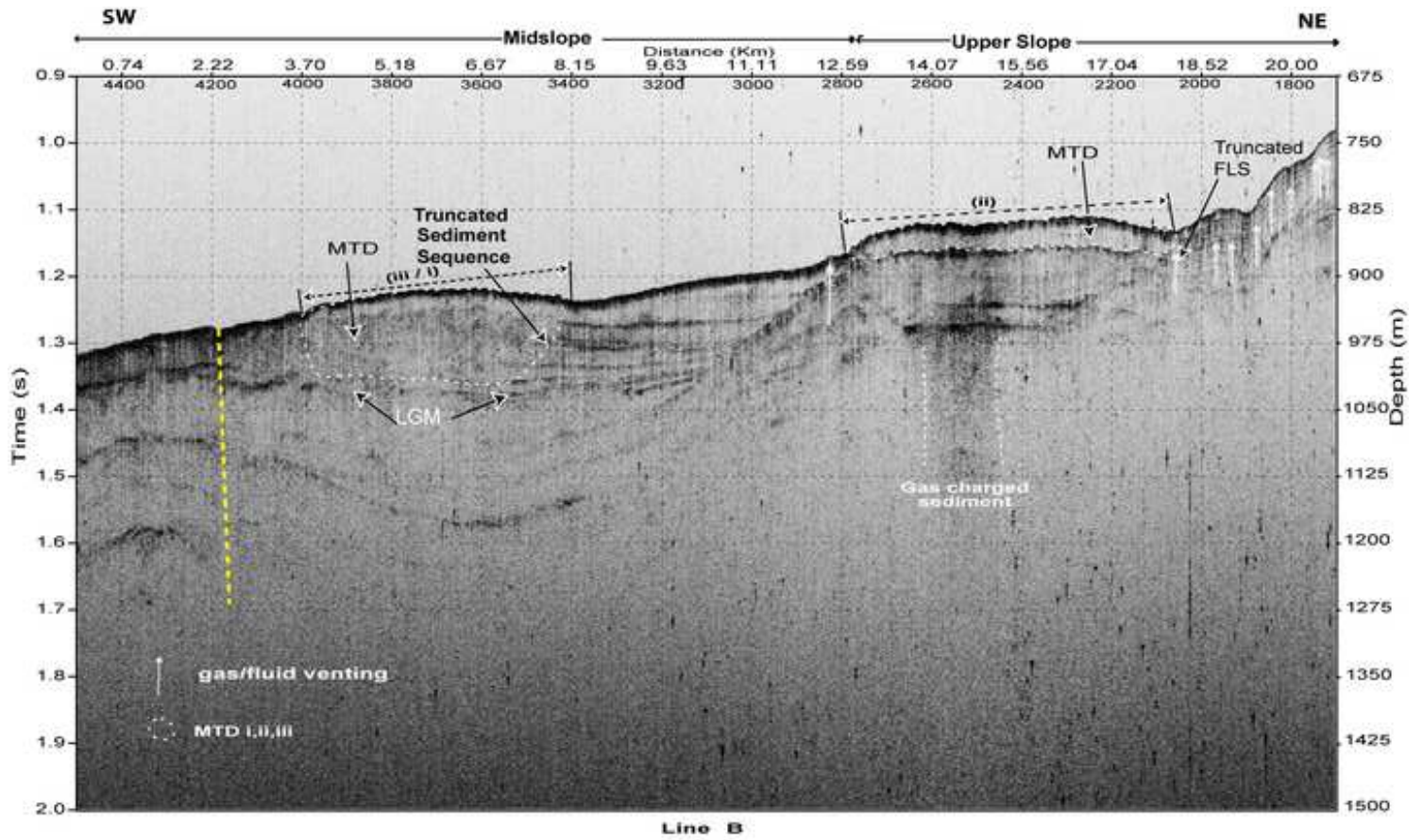


Fig.3b

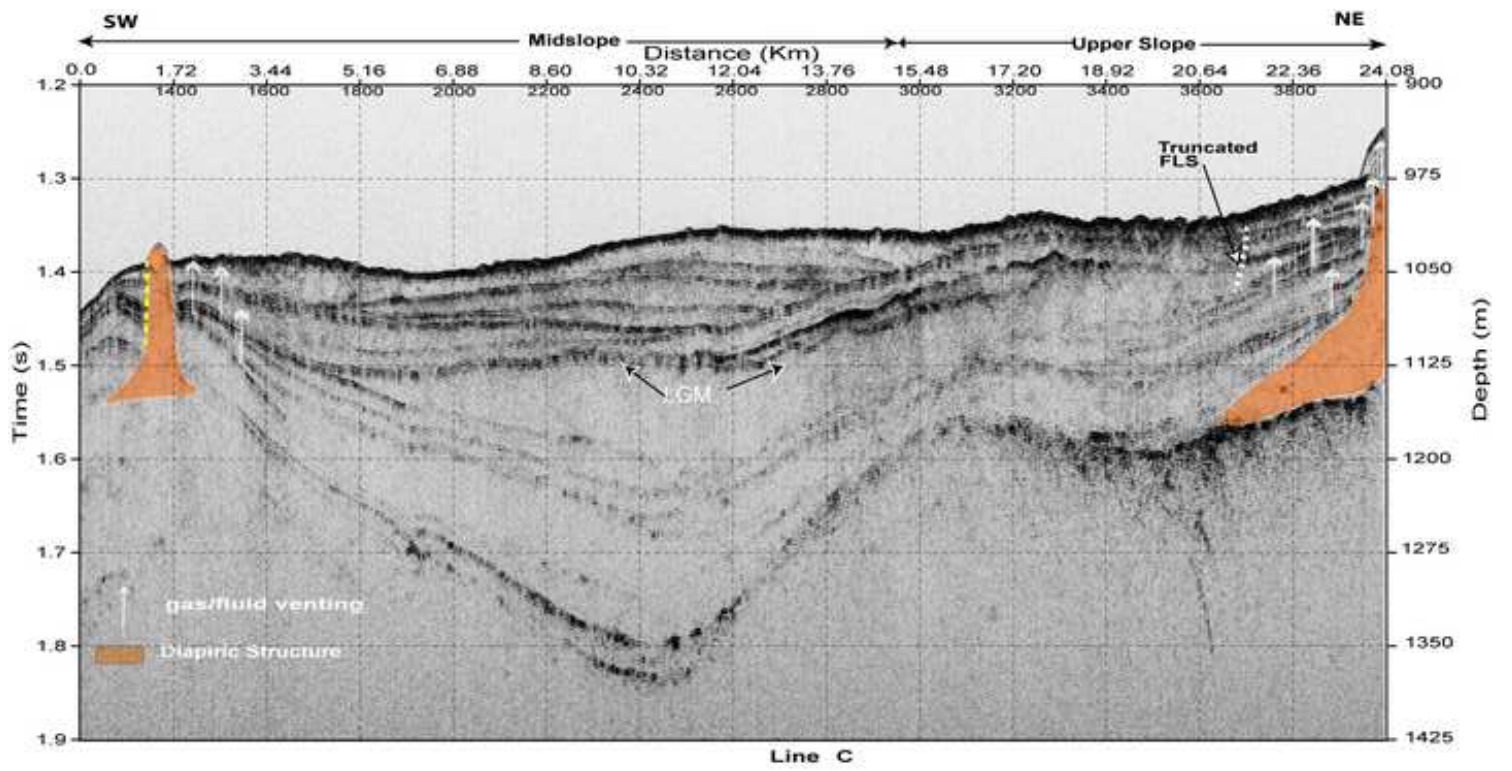


Fig.3c

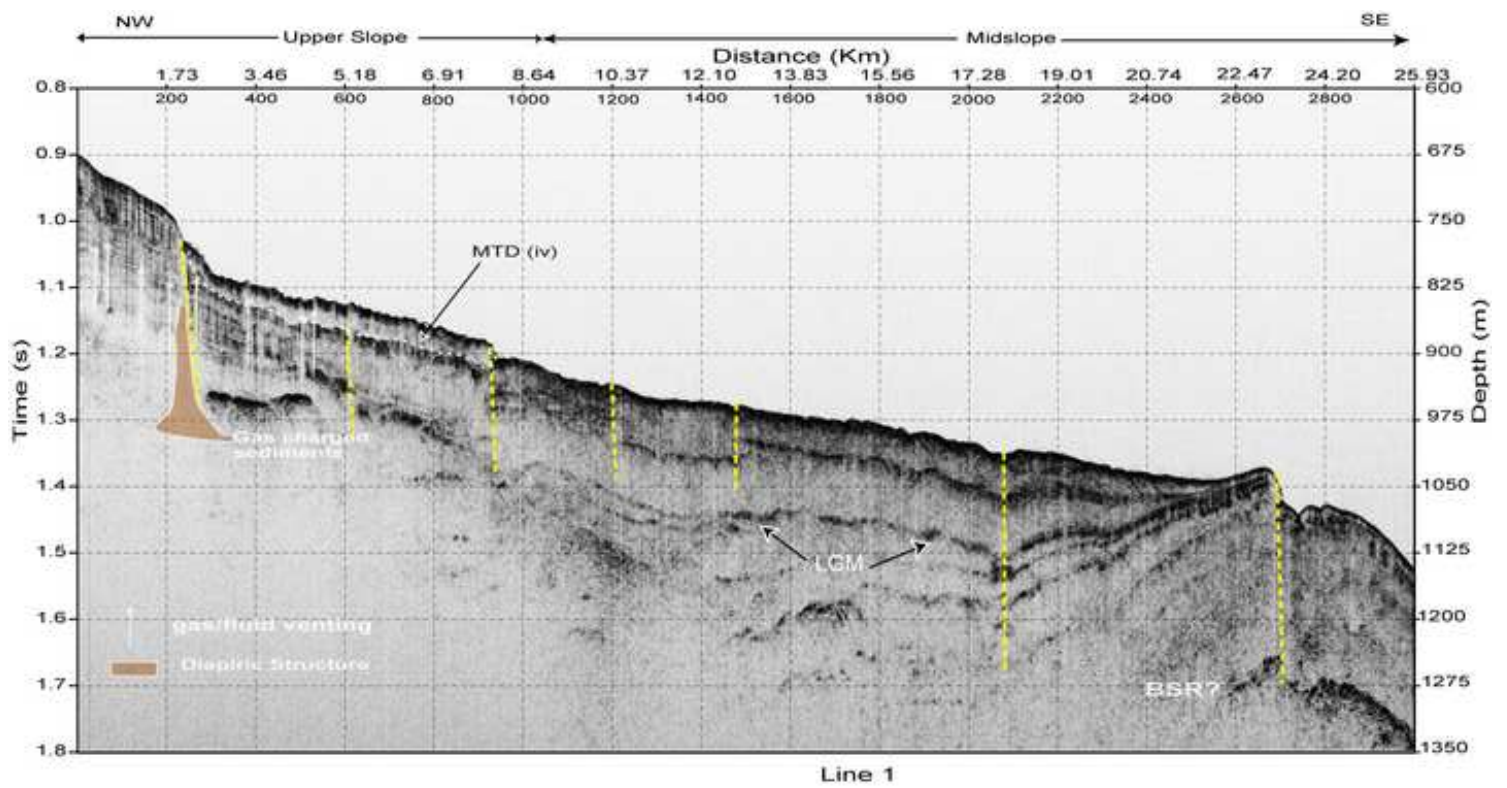


Fig.3d

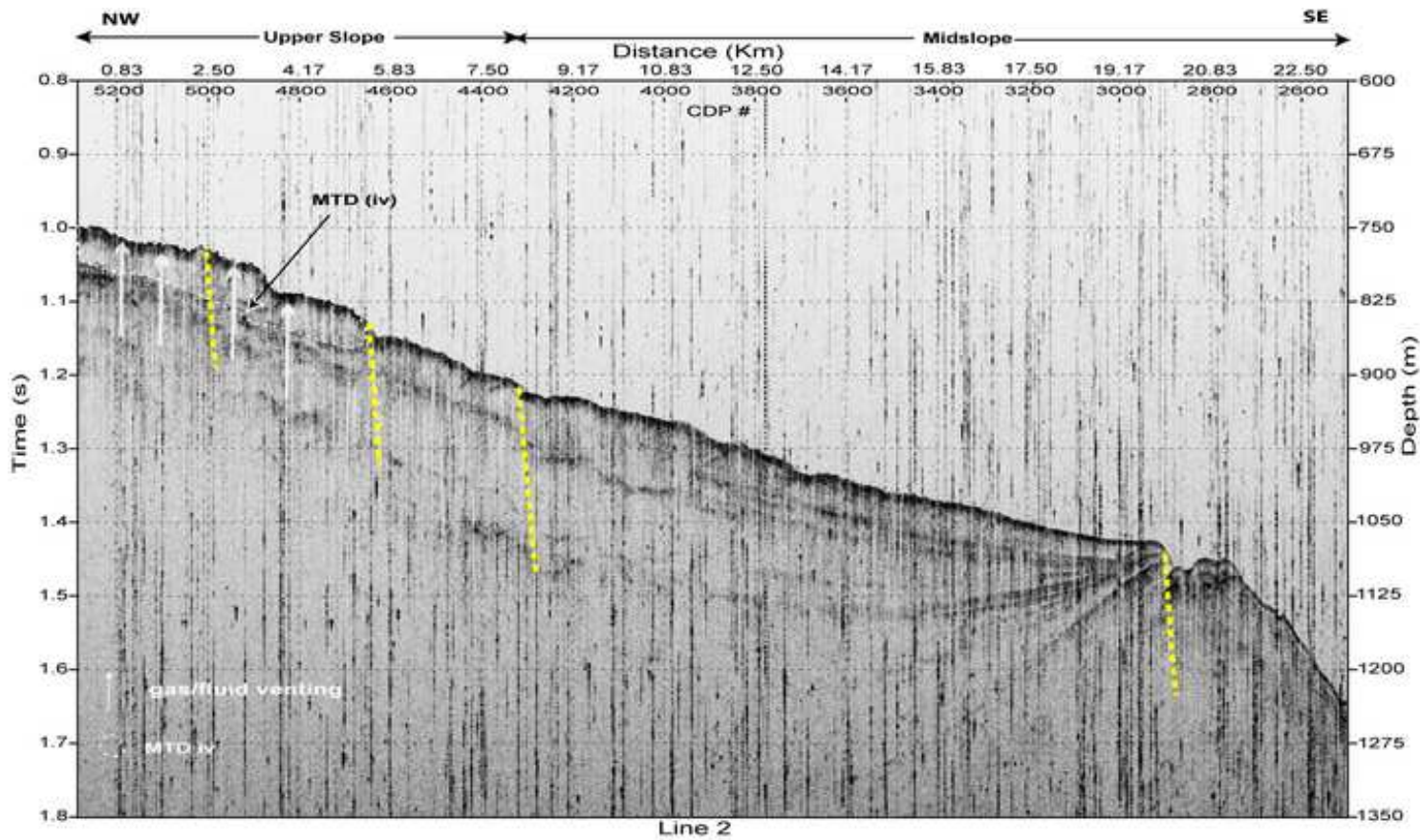
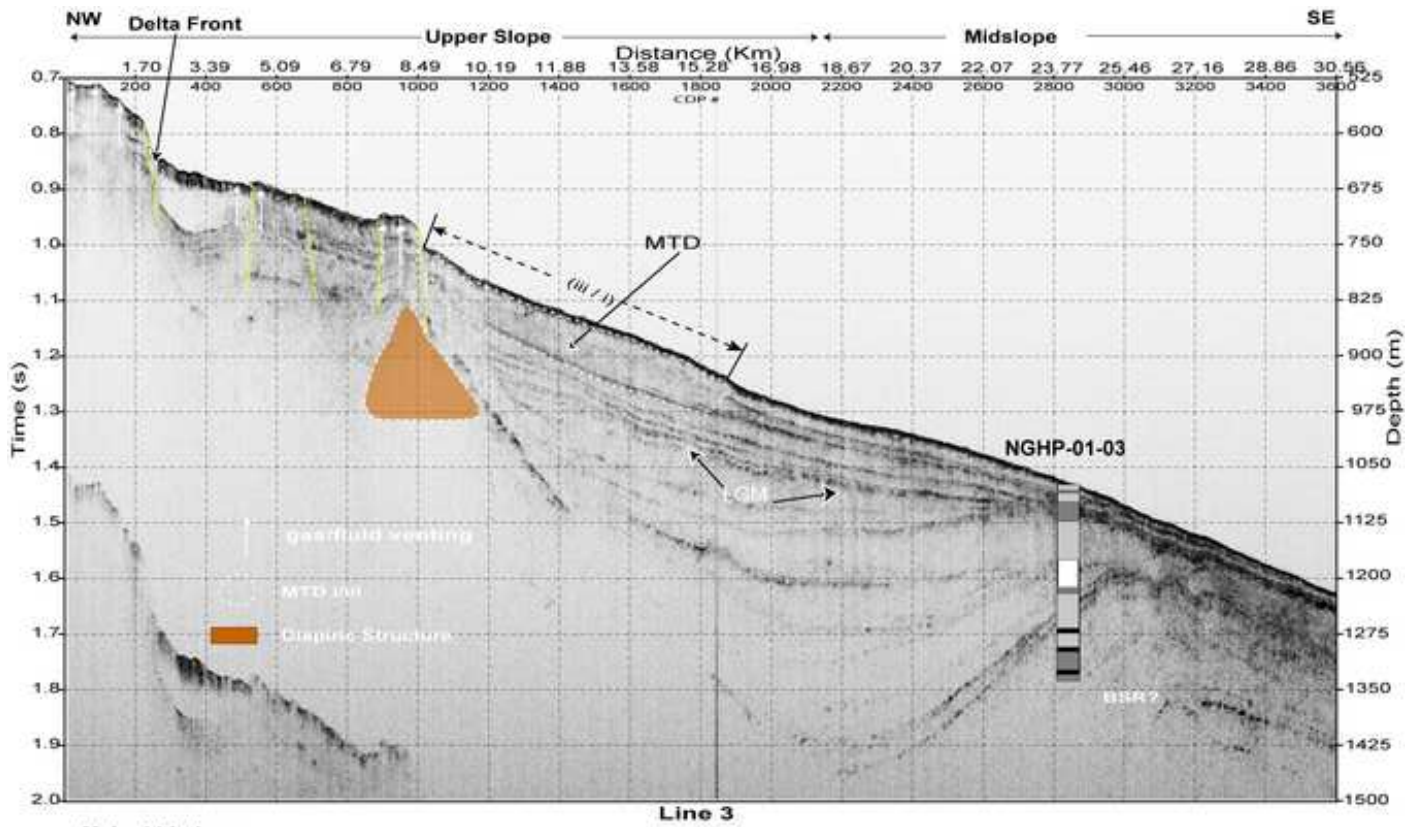


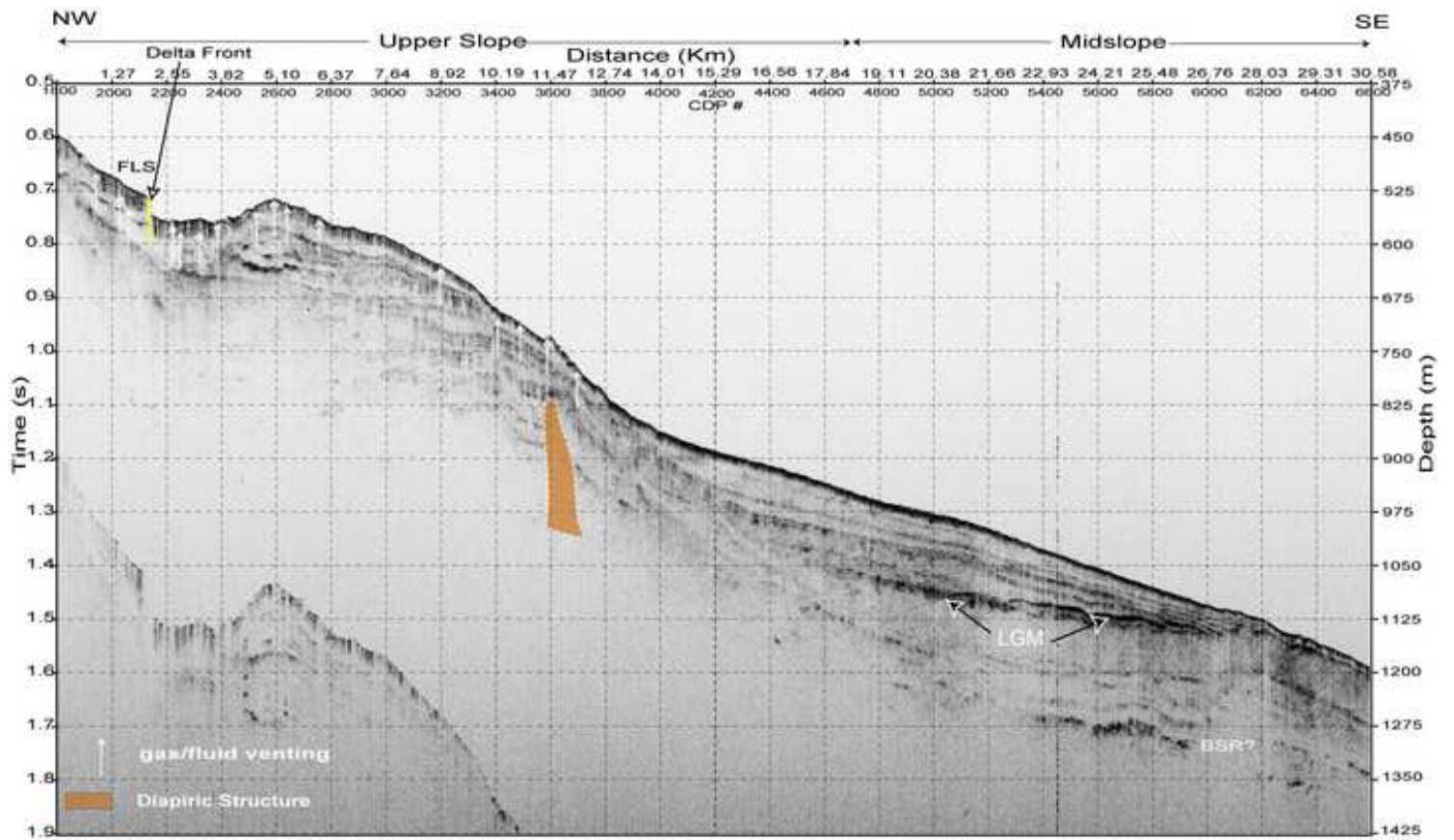
Fig.3e



Major Lithology

- Nannofossil bearing clay
- Nannofossil rich clay
- Foramanifera bearing clay
- No core recovery

Fig.3f



Line 4

Fig.3g

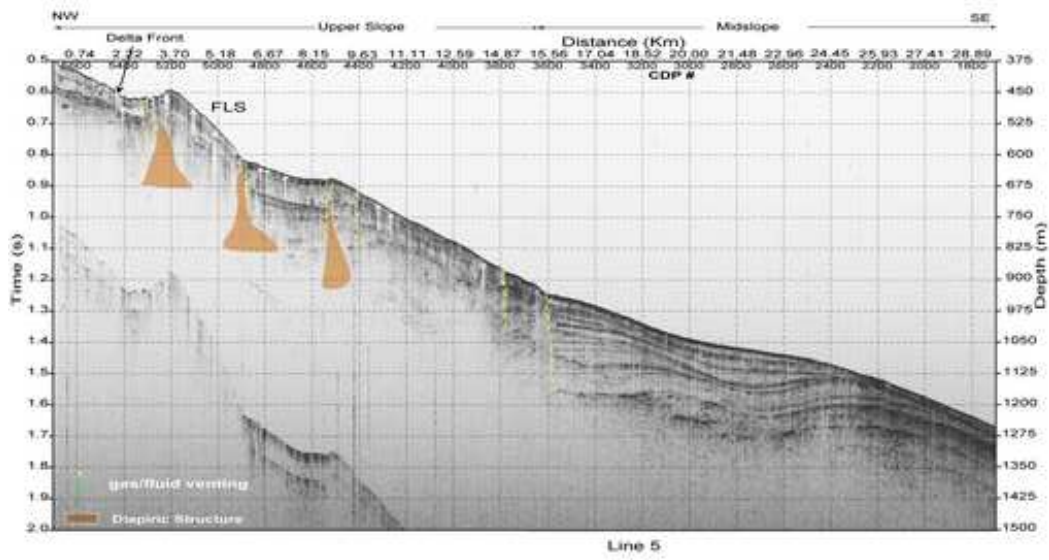
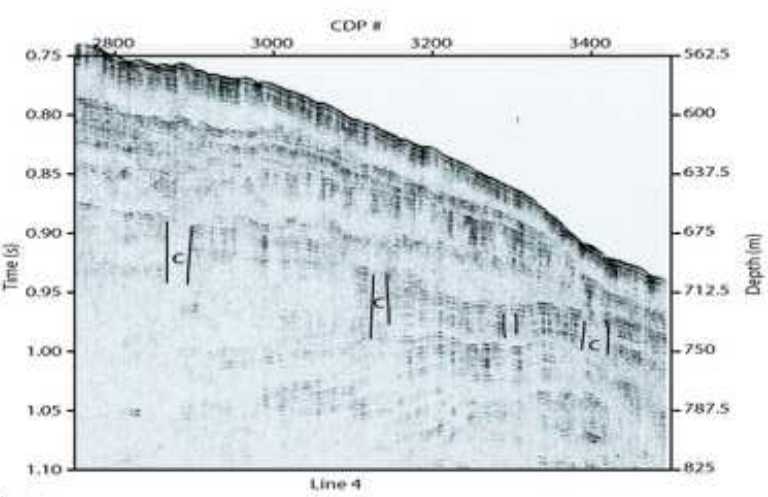
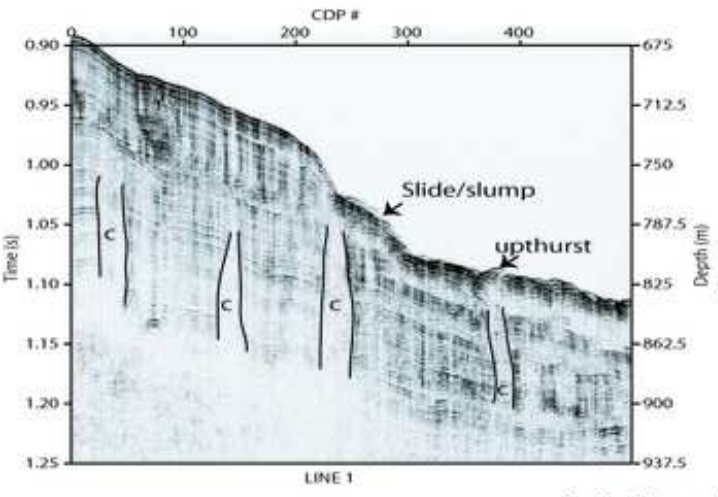
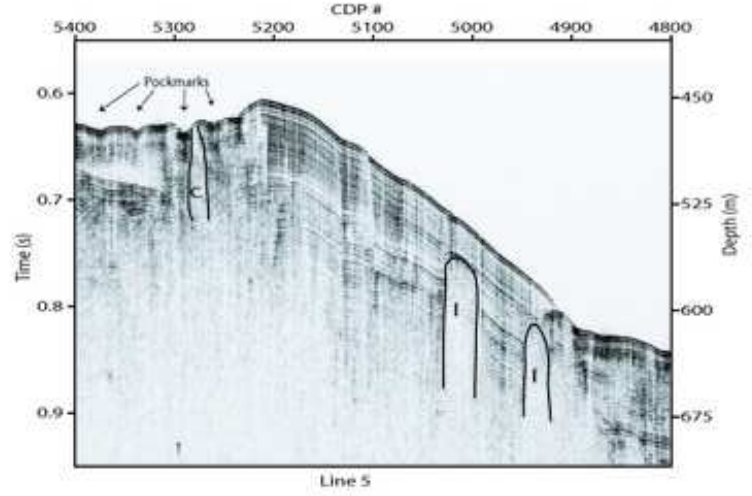
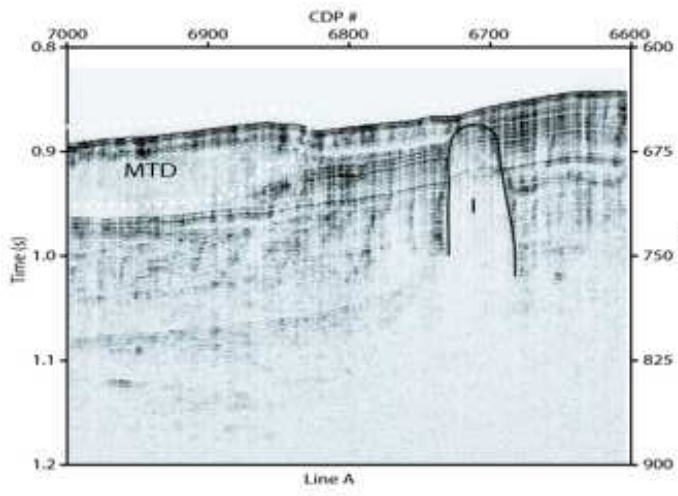


Fig.3h



C = Gas Chimneys/vents
 I = Inverted U-Shapes

Fig.4a

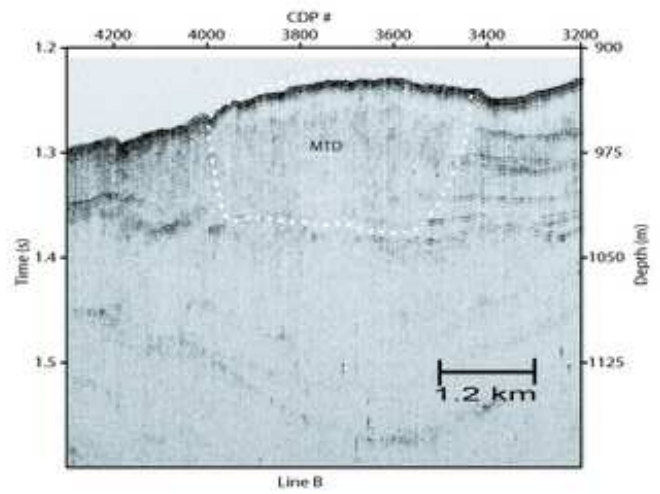
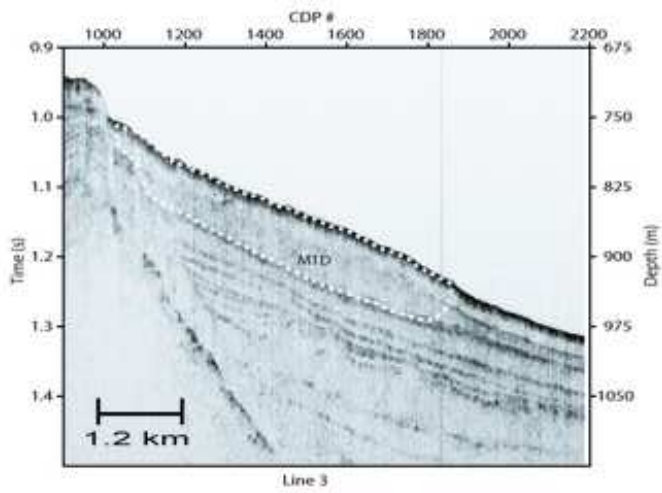
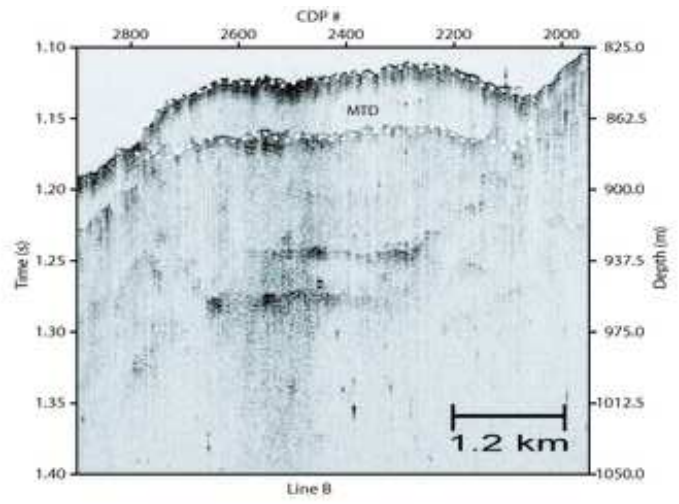
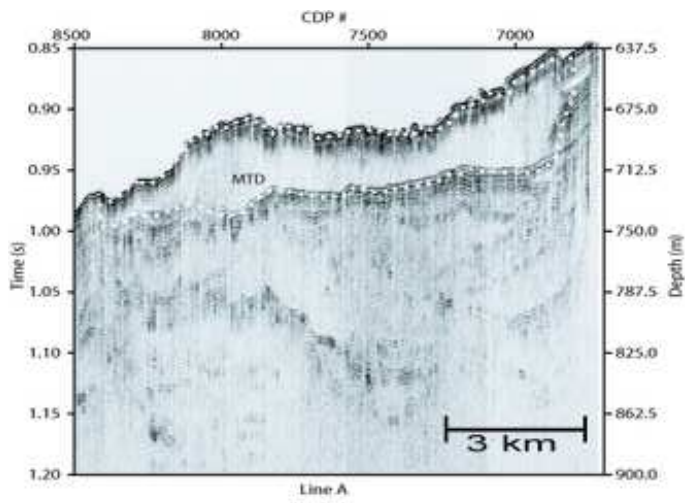


Fig. 4b

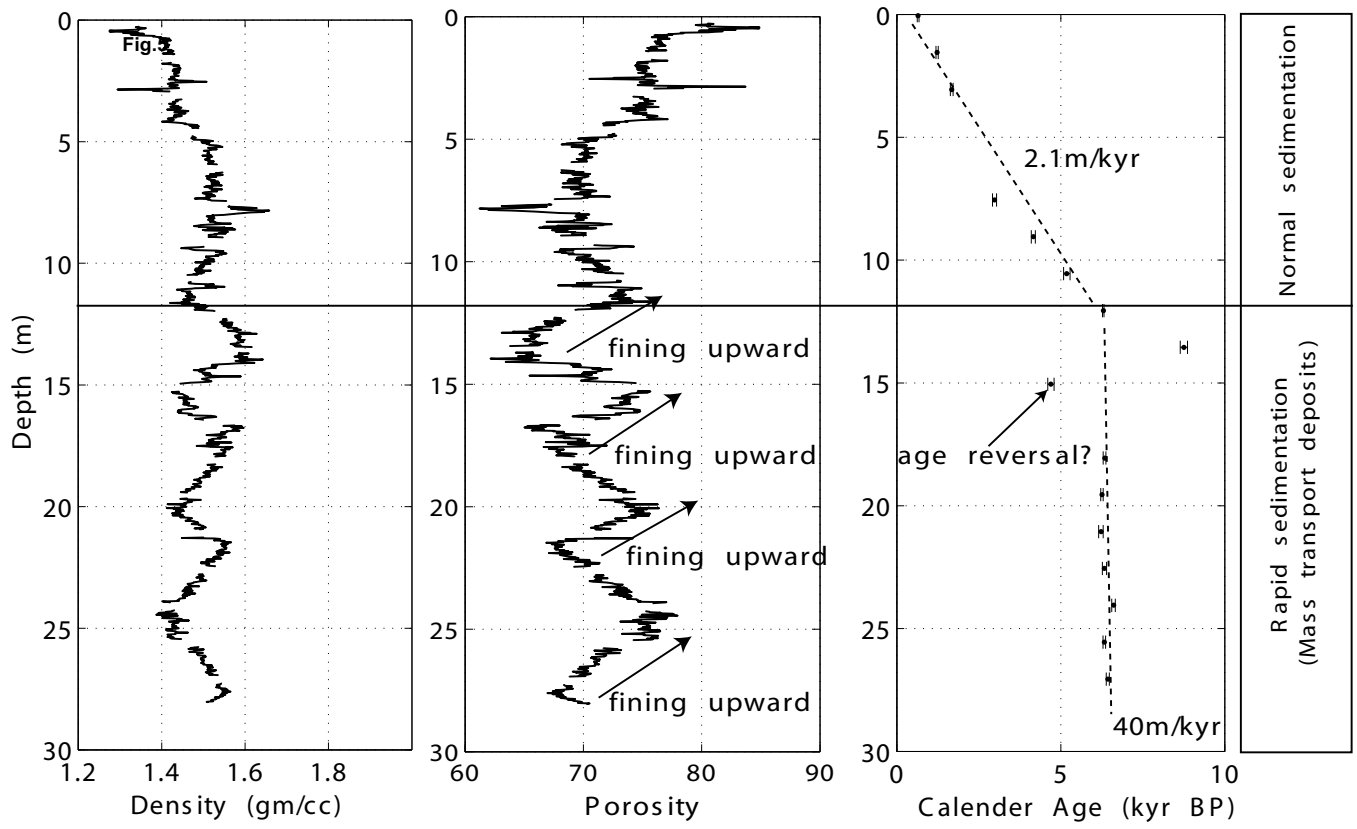


Fig.5

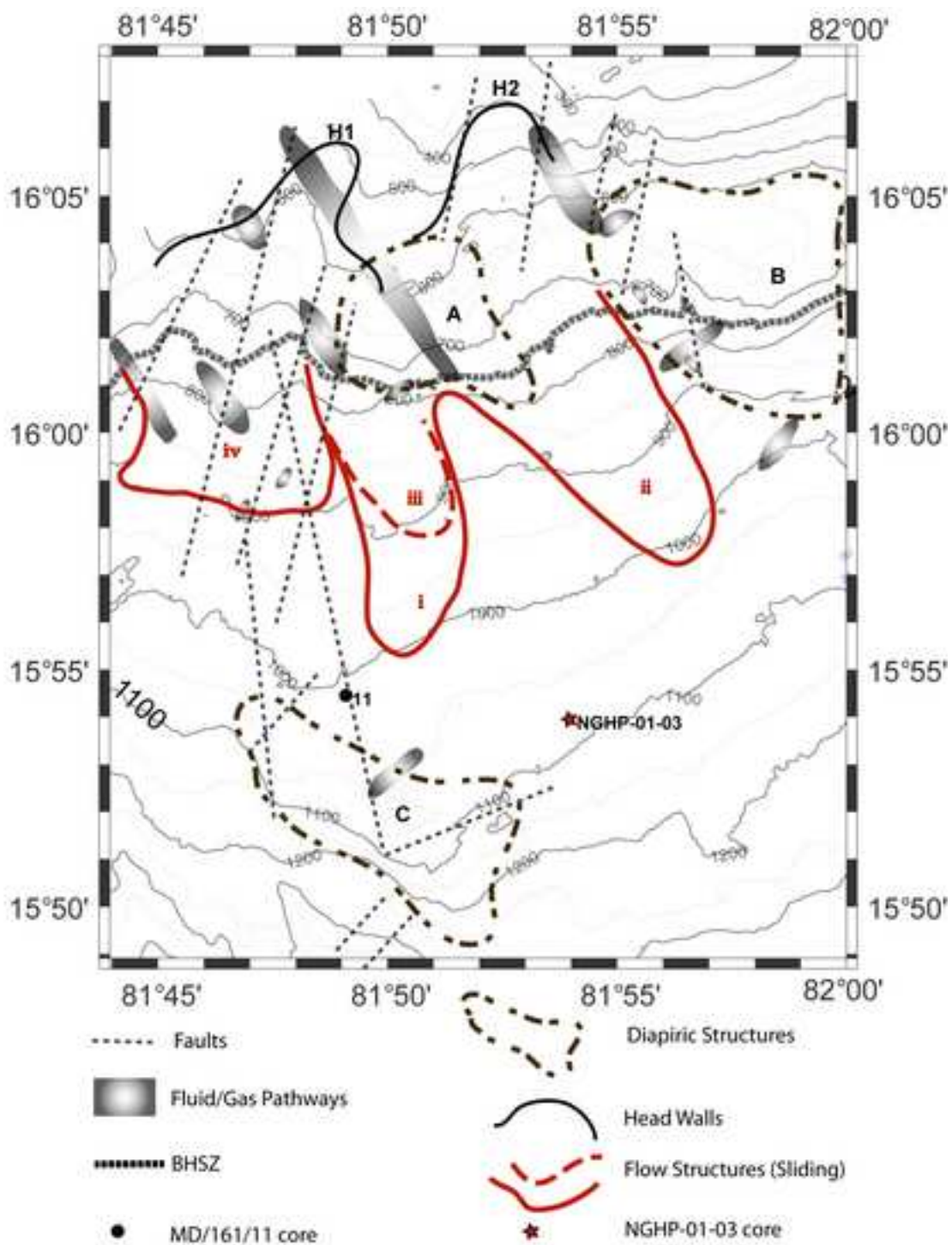


Fig.6

Table 1.

Sample No.	Depth (mbsf)	Calendar age (yr BP)	
		Mean	Std.dev.
MD161/11/1	0.05	648	27
MD161/11/2	1.55	1230	36
MD161/11/3	3.055	1677	42
MD161/11/6	7.55	2982	61
MD161/11/7	9.055	4163	63
MD161/11/8	10.55	5185	98
MD161/11/9	12.055	6296	24
MD161/11/10	13.55	8752	111
MD161/11/11	15.055	4700	98
MD161/11/13	18.055	6336	43
MD161/11/14	19.55	6258	37
MD161/11/15	21.055	6226	69
MD161/11/16	22.55	6333	66
MD161/11/17	24.055	6607	55
MD161/11/18	25.55	6327	41
MD161/11/19	27.055	6434	48